Electron Heating due to *S*-Polarized Microwave (Laser) Driven Parametric Instabilities

K. Mizuno and J. S. DeGroot
Department of Applied Science, University of California, Davis, California 95616

and

K. G. Estabrook
Lawrence Livermore National Laboratory, University of California, Livermore, California 94550

(Received 19 September 1983)

Microwave experiments and simulation calculations for laser parameters are reported of electron heating and microwave (laser) absorption due to parametric instabilities excited in the strongly steepened density profile near the critical surface. An approximate theory is developed that shows that T_H/T_e should be a function of only the variable $f_H I\lambda_0^2/T_e$. The microwave measurements and simulation calculation results agree (±20%) with this theory.

PACS numbers: 52.50.Jm, 52.25.Ps, 52.35.Py, 52.50.Gj

The use of high-power lasers to compress and heat a pellet to thermonuclear conditions is being intensely investigated. One of the crucial problems that strongly affects pellet performance is the generation of high-energy (hot) electrons due to resonance absorption[1] and parametric instabilities.[2] The ion-acoustic decay (IAD) instability,[3] in which the decay products are electron plasma waves and ion-acoustic waves, and the oscillating-two-stream (OTS) instability[3] have been shown[4] to produce hot electrons. Recently, Estabrook and Kruer[5] reported two-dimensional particle simulation calculations of normally incident laser light that show that parametric instabilities are important even in the strongly steepened plasma. In this Letter, we report results from microwave-driven experiments and particle simulation calculations that model *s*-polarized laser light–plasma interactions near the critical surface.

In the experiments, microwaves (frequency, $\omega_0/2 = 1.2$ GHz) are incident on an inhomogeneous plasma in a special section of *L*-band waveguide (height, $a = 8.25$ cm, and width, $b = 16.5$ cm; Fig. 1). This microwave-plasma interaction section is bounded transversely by the waveguide (constructed of high-transparency, conducting screen) and axially by a thin ceramic sheet (Fig. 1). The essentially collisionless ($\lambda_{en} \gtrsim 100$ cm), low-pressure (0.3 to 0.5 m Torr), argon plasma is produced in the microwave-plasma interaction section by primary electrons emitted from heated filaments. The microwaves are excited far (200 cm) from the microwave-plasma interaction section so that higher-order modes are damped and a well-defined TE_{10} mode is incident on the plasma.

The *s*-polarized microwaves are incident at an angle of about $\theta_{inc} \simeq 50°$ ($\sin\theta_{inc} = \lambda_0/2b$, where λ_0 is the microwave wavelength). Typical parameters are as follows: $n \lesssim 2n_c$, where n_c is the critical density, $n_c = 1.8 \times 10^{10}$ cm^{-3}; unperturbed electron temperature $T_{e0} \simeq 3$ eV; and electron to ion temperature ratio $T_{e0}/T_{i0} \simeq 10$. The maximum available microwave power is 5 kW (corresponding to $v_0/v_{e0} \simeq 0.7$). The microwave pulse length and argon gas pressure are adjusted so that plasma ionization due to hot electrons is negligible and yet suprathermal electron heating reaches nearly steady state (pulse width 2.5 to 10 μsec depending on the microwave power). The electrons heated along the electric field of the incident microwaves (y direction) are measured by an energy analyzer (Fig. 1). A small (diameter $\gtrsim \lambda_{De}$), coaxial, cylindrical Langmuir probe (Fig. 1) is used to measure the thermal electron temperature, the plasma density, and the relative high-frequency electric field strength. The microwave absorption coefficient $f \equiv P_{abs}/P_0$, is obtained from the difference between the measured values of the incident and the reflected microwave components (the transmitted component

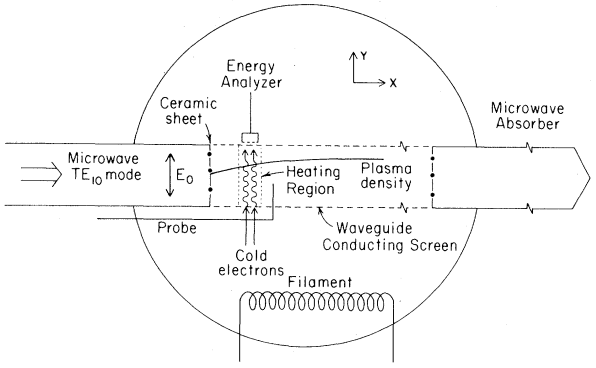

FIG. 1. Schematic of the experimental apparatus.

is negligibly small since the microwaves cannot propagate into the overdense region).

When the microwave power is above a well-defined threshold value, the simultaneous excitation of an ion wave (ω_i) and an electron plasma wave (ω_e) is observed.[6] Frequency conservation $\omega_0 \simeq \omega_e + \omega_i$ is satisfied between these waves. For weak microwave powers, only the Stokes satellite is observed, and the ion wave has a coherent (sinusoidal) temporal pattern. The ion wave frequency is typically 1 MHz (for microwave powers near threshold), indicating a wave number, $k\lambda_{De} \simeq 0.23$, which agrees with theory. Spatial correlation measurements indicate that the ion wave is propagating along the direction of the microwave electric field with approximately the sound speed. The spectral width of the electron plasma wave is large ($\Delta\omega/\omega_0 \gtrsim 3\% \gg \omega_{pi}/\omega_0$) for moderate-power microwaves [Fig. 2(a)].

For higher powers, where hot electrons are produced, we find that the density profile near the critical surface is strongly steepened[7] as a result of the ponderomotive force of the plasma waves, and the ion waves become turbulent.[8] The microwave absorption coefficient increases linearly with power in the weak power regime and is approximately constant at $f \simeq 20\%$ in the moderate power regime ($P_0 \gtrsim 0.2$ kW).

Figure 2(b) gives the electron current-voltage characteristic taken after the microwave-plasma interaction has reached steady state. A straight line on this graph indicates a Maxwellian energy distribution. Curve 1 shows the electron distribution without microwave power. The current of high-energy electrons increases with increasing microwave power (curve 2 to curve 4). The suprathermal electron distribution has a cutoff at a relatively low energy, $E_{cut} \simeq 25kT_{e0}$ (shown by the arrow on curve 2), for weak microwave powers. This cutoff energy does not depend strongly on microwave power in the weak power regime ($P_0 \lesssim 0.1$ kW, $v_0/v_{e0} \lesssim 0.1$). This cutoff velocity is on the order of the phase velocity of the most unstable waves [$v_{cut}/v_{ph} \lesssim (v_{cut}/v_{e0}) \times k\lambda_{De} \simeq 1.2$]. The measured steady-state hot-electron temperature is given closely by $T_H = 66P_0^{1/2}$ eV, where P_0 is the incident microwave power in kilowatts. Measurements of the thermal electron temperature taken inside the microwave-plasma interaction region show that the thermal electrons are also heated strongly, i.e., $T_e \simeq 9P_0^{0.4}$ eV. The measured ratio of hot to thermal electron temperature, T_H/T_e, is therefore a very slow function of microwave power, $T_H/T_e \simeq 7.3P_0^{0.1}$.

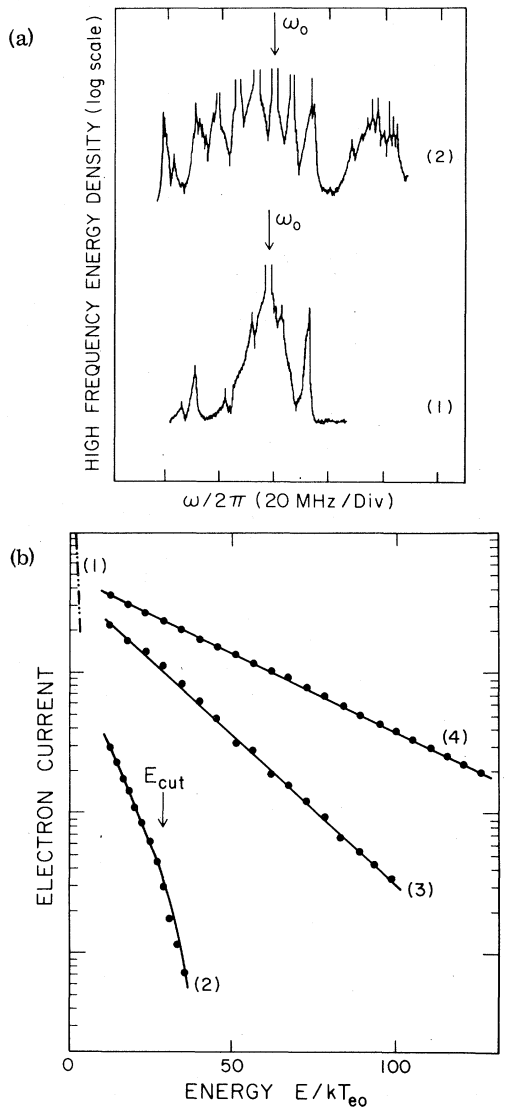

FIG. 2. (a) High-frequency spectrum well above threshold: curve 1, $P_0 = 0.43$ kW and curve 2, $P_0 = 1$ kW. (b) Electron current vs energy with microwave power as a parameter. All electrons with energy above the abscissa value are collected. Curves 1–4 correspond to microwave powers of 0, 50 W, 900 W, and 3 kW, respectively.

The computer simulation calculations are performed with use of the two-dimensional, relativistic, electromagnetic code ZOHAR[9] with 5×10^5 electrons and ions. The laser electric field is in the plane of the simulations. The light is normally incident onto a plasma with an initially linear density profile. The initial plasma density profile is chosen so that the ponderomotive force due to the high-frequency waves is almost in equilibrium with the force due to the pressure gradient.

The thermal electron temperature is typically $T_e \simeq 4$ keV, and $T_e/T_i \simeq 16$. The fractional absorption into hot electrons, f_H, is typically 11% to 17% due to the parametric instabilities (thermal-electron heating is negligible). High-energy electrons are strongly heated along the laser electric field (perpendicular to the density gradient). The electrons have a bi-Maxwellian energy distribution. The hot electron temperature is well represented by $T_H = 4.4\times10^{-4} I^{0.3}$ keV for $10^{15} \lesssim I \lesssim 10^{18}$ W/cm^2, and $T_e = 4$ keV.

We next develop an approximate theory. The basic idea[10] is to equate the fraction of the microwave (laser) power flux that produces hot electrons to the rate that the plasma waves heat the electrons, i.e.,

$$f_H I \simeq \int dx\, \nu_H \langle E_w^2(x)\rangle/8\pi, \tag{1}$$

where I is the incident microwave (laser) power flux, ν_H is the damping rate due to hot electron production, and $\langle E_w^2(x)\rangle^{1/2}$ is the rms amplitude of the electron-plasma-wave electric field. The unstable ion-acoustic waves are saturated as a result of ion trapping.[8] Thus, using the theory of the IAD instability,[2] we find that the saturated electron-plasma-wave electric field is

$$E_k \simeq (n_k/n_c)E_d/\epsilon_k, \tag{2}$$

where n_k is the amplitude of the ion wave with wave number k and ϵ_k is the dielectric for the electron plasma wave. Since E_k is sharply peaked near the critical density (because $|\epsilon_k(n \lesssim n_c)| \simeq \nu_H/\omega_0 \ll 1$), we assume that n_k and ν_H are independent of position. The integral in Eq. (1) can be performed [for a linear density profile, $n(x) = n_c(x/L)$], and Eq. (1) is solved for ν_H to obtain

$$\frac{\nu_H}{\omega_0} \simeq \left(\frac{8}{\eta_w^2 L/\lambda_{De}}\,\frac{f_H I}{n_c v_e T_e}\right)^{1/2}, \tag{3}$$

where $\eta_w^2 = \langle E_w^2\rangle_{\max}/4\pi n_c k T_e$, and T_e is the thermal electron temperature. The damping coefficient, ν_H, is just due to Landau damping of the hot electrons evaluated at the phase velocity of the most unstable wave ($k\lambda_{De} \simeq \frac{1}{4}$). A direct calculation gives $\nu_H/\omega_0 \simeq 3n_H/n_c$, where n_H is the hot electron density.

We can obtain another equation for n_H by equating the flux of hot electrons to the absorbed power, i.e.,

$$f_H I = 2 n_H v_H k T_H \langle\cos\theta\rangle, \tag{4}$$

where $v_H = kT_H/m$, θ is the angle between a heated electron and the x axis (Fig. 1), and the factor of 2 comes about because the electrons are heated in the $\pm y$ directions. Since the electrons are predominantly heated in the $\pm y$ directions, we assume $\langle\cos\theta\rangle \simeq \frac{1}{2}$. Combining Eqs. (3) and (4) (with $\nu_H/\omega_0 \simeq 3n_H/n_c$), we obtain

$$\frac{T_H}{T_e} \simeq (4\pi)^{1/3}\left(\frac{f_H I}{n_c v_e T_e}\right)^{1/3}\left(\frac{\eta_w^2 L}{\lambda_{De}}\right)^{1/3}. \tag{5}$$

The density scale length near the critical surface, L, is determined by the balance between the ponderomotive force and the plasma pressure force. In the microwave experiments, we find $\eta_w^2 L/\lambda_{De} \simeq 50$, almost independent of power (for high enough powers that hot electrons are produced). An approximate theory gives $\eta_w^2 L/\lambda_{De} \simeq 60$ (for $T_e/T_i \simeq 1$) and 20 (for $T_e/T_i \gg 1$). Using these results in Eq. (5), we obtain

$$T_H/T_e \simeq A\times10^{-4}(f_H I \lambda_0^2/T_e^{3/2})^{1/3}, \tag{6}$$

where $A \simeq 1.4$ for $T_e/T_i \simeq 1$ and $A \simeq 1.0$ for $T_e/T_i \gg 1$, and the units are I(W/cm^2), $\lambda_0(\mu$m), and T_e(keV).

The hot electron temperatures from the microwave experiments and from the simulation calculations for laser parameters are shown in Fig. 3 as a function of this variable. Note that the close agreement between these two sets of results is strong evidence that $f_H I\lambda_0^2/T_e$ is a universal variable. The theoretical predictions

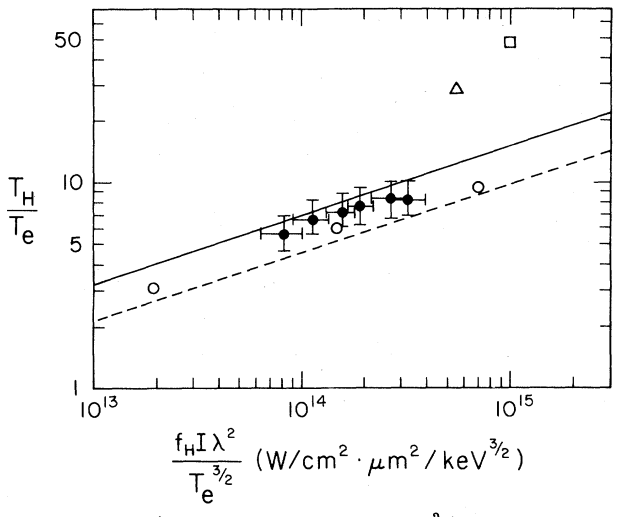

FIG. 3. T_H/T_e as a function of $f_H I\lambda_0^2/T_e$. The solid circles are microwave measurements and the open circles are simulation results. The solid line is the theoretical prediction [Eq. (6)] for $T_e/T_i = 1$ and the dashed line is for $T_e/T_i \gg 1$. The triangle and the square are simulation results for long (non-self-consistent) plasma density scale lengths ($L/\lambda_{De} \simeq 6.7\times10^2$ and $\simeq 1.1\times10^3$) with the same laser intensity as for the open circle shown at the center.

[Eq. (6)] are also shown in Fig. 3. In the microwave experiments, the ions are heated strongly[8] and $T_i \lesssim T_e$ so that the microwave measurements should be compared to the $T_e/T_i = 1$ prediction. The temperature ratio is large in the simulation calculations so that the simulation results should be compared to the $T_e/T_i \gg 1$ prediction. We see good ($\pm 20\%$) agreement between theory, microwave measurements, and simulation calculations for laser parameters.

These results only apply to the case that the density profile is self-consistently determined by the ponderomotive force. Simulation calculations with shallow density profiles that are not in force equilibrium give quite different results (triangle and square in Fig. 3).

In summary, we have presented microwave measurements and simulation calculations for laser parameters of electron heating and microwave (laser) absorption due to parametric instabilities excited in the strongly steepened density profile near the critical surface by s-polarized microwaves (laser light). An approximate theory is developed that shows that T_H/T_e should be a function of only the variable $f_H I\lambda_0^2/T_e$. The microwave measurements and simulation results agree ($\pm 20\%$) with this theory. These results also are comparable with hot-electron generation[10] due to resonance absorption of p-polarized microwaves[11] (laser light[12]), over the parameter range that we have investigated.

We are grateful to W. L. Kruer for many valuable discussions. The expert assistance of T. Hillyer is gratefully acknowledged. This work was supported by the Lawrence Livermore National Laboratory.

[1]V. Ginzburg, *Propagation of Electromagnetic Waves in Plasma* (Gordon and Breach, New York, 1961), p. 377ff.

[2]C. S. Liu, in *Advances in Plasma Physics*, edited by A. Simon and W. Thompson (Wiley, New York, 1976).

[3]D. F. DuBois and M. V. Goldman, Phys. Rev. 164, 107 (1967); K. Nishikawa, J. Phys. Soc. Jpn. 24, 916, 1152 (1968); F. W. Perkins and J. Flick, Phys. Fluids 14, 1012 (1971).

[4]T. K. Chu and H. W. Hendel, Phys. Rev. 29, 634 (1972); H. Dreicer, R. F. Ellis, and J. C. Ingraham, Phys. Rev. Lett. 31, 426 (1973).

[5]K. G. Estabrook and W. L. Kruer, Phys. Fluids 26, 1888 (1983).

[6]K. Mizuno and J. S. DeGroot, Phys. Rev. Lett. 35, 219 (1975).

[7]K. Mizuno and J. S. DeGroot, Phys. Fluids 22, 2229 (1979).

[8]K. Mizuno and J. S. DeGroot, Phys. Fluids 26, 608 (1983).

[9]A. B. Langdon and B. F. Lasinski, in *Methods in Computational Physics*, edited by J. Kileen (Academic, New York, 1976), Vol. 16.

[10]J. S. DeGroot, W. L. Kruer, Wee Woo, and K. Mizuno, University of California at Davis Report No. PRG-R-48 (to be published).

[11]K. Mizuno and J. S. DeGroot, and F. Kehl, Phys. Rev. Lett. 49, 1004 (1982).

[12]D. W. Forslund, J. M. Kindel, and K. Lee, Phys. Rev. Lett. 39, 284 (1977); K. G. Estabrook and W. L. Kruer, Phys. Rev. Lett. 40, 42 (1978).